Active disturbance rejection control for small unmanned helicopters via Levy flight-based pigeon-inspired optimization

Daifeng Zhang, Haibin Duan and Yijun Yang
Science and Technology on Aircraft Control Laboratory, Beihang University, Beijing, China

Abstract
Purpose – The purpose of this paper is to propose a control approach for small unmanned helicopters, and a novel swarm intelligence algorithm is used to optimize the parameters of the proposed controller.
Design/methodology/approach – Small unmanned helicopters have many advantages over other unmanned aerial vehicles. However, the manual operation process is difficult because the model is always instable and coupling. In this paper, a novel optimized active disturbance rejection control (ADRC) approach is presented for small unmanned helicopters. First, a linear attitude model is built in hovering condition according to small perturbation linearization. To realize decoupling, this model is divided into two parts, and each part is equipped with an ADRC controller. Finally, a novel Levy flight-based pigeon-inspired optimization (LFPIO) algorithm is developed to find the optimal ADRC parameters and enhance the performance of controller.
Findings – This paper applies ADRC method to the attitude control of small unmanned helicopters so that it can be implemented in practical flight under complex environments. Besides, a novel LFPIO algorithm is proposed to optimize the parameters of ADRC and is proved to be more efficient than other homogenous methods.
Research limitations/implications – The model of proposed controller is built in the hovering action, whereas it cannot be used in other flight modes.
Practical implications – The optimized ADRC method can be implemented in actual flight, and the proposed LFPIO algorithm can be developed in other practical optimization problems.
Originality/value – ADRC method can enhance the response and robustness of unmanned helicopters which make it valuable in actual environments. The proposed LFPIO algorithm is proved to be an effective swarm intelligence optimizer, and it is convenient and valuable to apply it in other optimized systems.

Keywords Parameter optimization, Active disturbance rejection control, Levy flight-based pigeon-inspired optimization, Small unmanned helicopters

Paper type Research paper

Introduction

As a common type of unmanned aerial vehicles (UAVs), unmanned helicopters overcome many obstacles in UAV flight. For example, when implementing rescue or other critical missions, it is always necessary for UAVs to hover in the air. However, the wing aircrafts cannot finish. On the contrary, unmanned helicopters could complete a variety of special actions including hover; therefore, it's easy to execute these critical missions. However, the operation process is hard for helicopter pilots because of its instable and nonlinear coupling model. Hovering flight is an important action for small unmanned helicopters in many emergences, and it has aroused interests among scholars to study the model in hovering flight. To realize autonomous flight, it is important to design high-performance attitude controller. In recent years, there are a lot of proposed advanced control methods for unmanned helicopters, such as the H_∞ method (Cai *et al.*, 2011; Ismaila *et al.*, 2011), backstepping (Lu *et al.*, 2015), adaptive control (Sheng *et al.*, 2014), fuzzy control (Ho *et al.*, 2008) and artificial intelligence (Nodland *et al.*, 2013). Nevertheless, these methods are rarely applied in practical engineering because of their complicated structure and high requirement to computing device. Active disturbance rejection control (ADRC) (Tang *et al.*, 2015) stems from proportional–integral–derivative controller (PID controller) algorithm; thus, it does not need high computation power and the exact object model. Besides, ADRC modifies the traditional PID structure and solves the inherent contradiction between overshoot and rise time in PID, which provides precise performance and high robustness simultaneously.

The parameters of ADRC are usually adjusted by some empirical formula (Han, 2009) and cannot be changed during the flight process. But sometimes we need to adjust parameters dynamically to make them adaptable. Hence, a parameter optimizing strategy is needed. Traditional parameter optimizing

The current issue and full text archive of this journal is available on Emerald Insight at: **www.emeraldinsight.com/1748-8842.htm**

Aircraft Engineering and Aerospace Technology: An International Journal
89/6 (2017) 946–952

[DOI 10.1108/AEAT-05-2016-0065]

This work was partially supported by National Natural Science Foundation of China under grant No. 61425008, 61333004 and 61273054 and Aeronautical Foundation of China under grant No. 2015ZA51013.

Received 2 May 2016
Revised 14 May 2016
15 May 2016
Accepted 17 May 2016

methods include critical proportion method (An *et al.*, 2015), attenuation curve method (Bassrei and Santos, 2007) and Ziegler–Nichols formula (Kushwah and Patra, 2014). However, these strategies are too complex to be used in practical tuning and easy to produce high frequency vibration. Recently, swarm intelligence techniques (Qiu *et al.*, 2015) have been concerned in the parameter optimization problems. Particle swarm optimization (PSO) (Duan *et al.*, 2013; Shi *et al.*, 2008) is a kind of swarm intelligence optimizer, which imitates the migration and foraging process of bird swarms. It is equipped with simple computation structure and prone to search global optima for complicate and multi-dimension problems. But the shortcomings of PSO are also obvious: It is easy to fall into the locally optimal solution and limited to premature convergence. Pigeon-inspired optimization (PIO) algorithm is a new bio-inspired swarm optimizer (Deng and Duan, 2016; Duan and Qiao, 2014; Duan and Wang, 2016; Zhang and Duan, 2016) which imitates the process of homing pigeons finding paths. Some new studies (Duan and Qiao, 2014) demonstrate that it can provide wider search space and faster convergence speed than many other advanced algorithms and is easier to obtain the globally optimal solution.

Composition and modeling of small unmanned helicopter

The basic composition of a small unmanned helicopter mainly consists of such three components as the main rotor, the fuselage and the tail rotor. The main rotor is responsible for the ascension and turning, which ensures to provide enough elevating force for flight. Therefore, the main rotor is the uppermost constituent, whereas its dynamic characteristics are very complicated. Meanwhile, in some cases such as high speed movement and large maneuver, the aerodynamics of fuselage are usually less certain. But in this paper, we mainly discuss the hovering state in actual flight which only permits low forward speed and little flexibility. Thus, the main rotor dynamics are simpler to determine and the fuselage dynamics can be neglected. Tail rotor is used to balance the torque force produced by main rotor and is responsible for the yaw actions. Due to instability of the tail system, an angular vector control system (AVCS) is used to stabilize the yaw channel which is a closed-loop subsystem based on PID controller (Yang *et al.*, 2013). Figure 1 shows the model helicopter in this paper.

Figure 1 Small unmanned helicopter Trex600E

The mathematical model of small unmanned helicopters is surely nonlinear, highly coupling and time-variant. But in many cases as above, we are interested to study the hovering state in which the lift force is almost equal to gravity. In condition of hovering state, we can extract a linear model for small unmanned helicopters through small perturbation linearization (Cao *et al.*, 2004; Ismaila *et al.*, 2011). Normally, a small unmanned helicopter is assembled with four digital servos so that the system inputs contain four channels as lateral channel, longitudinal channel, height channel and yaw channel. Each channel is responsible for control to the corresponding subsystem. The height and yaw subsystems with AVCS are regarded as independent first-order model, and they are easy to operate (Yang *et al.*, 2013). On the other hands, lateral and longitudinal attitude models are complicated and coupled. Therefore, we mainly focus on the modeling and control for these two subsystems. According to the characteristics of hovering state, the magnitude of main rotor lift force is almost equal to the gravity, and its direction is determined by a and b which define the tilting angle of the rotor tip-path-plane (TPP) in longitudinal and lateral directions (Tang *et al.*, 2014). Taken together, the moments of main rotor can be described as:

$$\begin{aligned} L_{mr} &\approx (k_\beta + mgH)b \\ M_{mr} &\approx (k_\beta + mgH)a \end{aligned} \tag{1}$$

where k_β defines the spring constant of the rotor hub, and H is the geometric parameter of fuselage. According to the small perturbation linearization, the angular velocity p in longitudinal channel and q in lateral channel are proportional to the relative moments and tilting angles of TPP. According to some studies (Tang *et al.*, 2014), the states a and b are approximate to first-order models and can be directly controlled by the system inputs$[\delta_{lat}, \delta_{lon}]$. Thus, we obtain the linear model of small unmanned helicopters as following equations:

$$\dot{x} = \mathbf{A}x + \mathbf{B}u$$

$$\mathbf{A} = \begin{bmatrix} 0 & 0 & 0 & L_b \\ 0 & 0 & M_a & 0 \\ 0 & -1 & -1/\tau & A_b \\ -1 & 0 & B_a & -1/\tau \end{bmatrix} \mathbf{B} = \begin{bmatrix} 0 & 0 \\ 0 & 0 \\ A_{lat} & A_{lon} \\ B_{lat} & B_{lon} \end{bmatrix} \tag{2}$$

where $\boldsymbol{x}$ defines the state variables as $[p, q, a, b]$; $\boldsymbol{u}$ is the system inputs as$[\delta_{lat}, \delta_{lon}]$; L_b, M_a are the differential operators to relative states; andτ defines the time constant of delay for tilting angles of TPP.

From the system matrix $\mathbf{A}$, we can conclude that state variables a and b are similar to second-order differentials to attitude angles and are directly relative to the system inputs $\boldsymbol{u}$. Because a and b are difficult to observe, some advanced control laws are not suitable for this system. Besides these two channels obviously exist cross coupling, which is troublesome for system running.

Active disturbance rejection control

ADRC is based on the classical PID algorithm. It succeeds some advantages of PID, such as the concept of using error to remove error. In addition, ADRC revises some drawbacks of PID and enhances the performance. The contradictions between the overshoot and search speed always impede the performances of the classical PID algorihtm. ADRC solves this problem with the component tracking differential (TD) and provides effectiveness and robustness through nonlinear state feedback (NLSEF) and extended state observer (ESO) (Han, 2009). Figure 2 shows the structure of our ADRC.

TD is used to trace the command input v_c and configure the transition process by introducing transition reference v_1 and its differential v_2. TD obviously slows down the fierce change of error and provides a smooth and steady transition. The structure of TD is described as:

$$\begin{cases} fh = fhan(v_1 - v_c, v_2, r_0, h) \\ v_1 = v_1 + h \cdot v_2 \\ v_2 = v_2 + h \cdot fh \end{cases} \tag{3}$$

where the function *fhan* is the optimal control synthesis function, which derives from the discrete optimization theory (Han, 2009). h and r_0 denotes the step length and the speed constant of convergence. The iteration process of optimal control synthesis function are given as follows:

$$u = fhan(x_1, x_2, r, h): \begin{cases} d = rh \\ d_0 = rh^2 \\ y = x_1 + hx_2 \\ a_0 = \sqrt{d^2 + 8r|y|} \\ a = \begin{cases} x_2 + \dfrac{(a_0 - d)}{2} sign(y) & , |y| > d_0 \\ x_2 + \dfrac{y}{h} & , |y| \le d_0 \end{cases} \\ u = -\begin{cases} r \cdot sign(y) & , |a| > d \\ r\dfrac{a}{d} & , |a| \le d \end{cases} \end{cases} \tag{4}$$

where $sign(x)$ denotes the sign function.

Unlike traditional PID, ADRC introduces NLSEF to promote the efficiency of control inputs via some nonlinear combinations of system errors. ESO is essential for stability and robustness, which not only gives the precise observation of system variables through z_1 and z_2 but also provides the real-time unknown dynamics prediction through z_3. So we can use ESO to compensate the unwanted changes by following equation:

$$u = u_0 - z_3 \tag{5}$$

This process denotes feedback linearization. u_0 is the NLSEF output that represents the ideal control without considering unknown dynamics. When we compensate the practical control u by subtracting unknown dynamics z_3 from u_0, the original system is equivalent to a second-order integrator system with ideal control. Thus, the original model is decoupled. The flow of ESO computation is given as follows:

$$\begin{cases} e = z_1 - y \\ fe = fal(e, 0.5, h),\ fe_1 = fal(e, 0.25, h) \\ \dot{z}_1 = z_2 - \beta_{01} e \\ \dot{z}_2 = z_3 - \beta_{02} fe + u \\ \dot{z}_3 = -\beta_{03} fe_1 \end{cases} \tag{6}$$

where y denotes the system output. The nonlinear function *fal* features fast tracking, and the structure is given as:

$$fal(e, \alpha, \delta) = \begin{cases} \dfrac{e}{\delta^{1-\alpha}}, |e| \le \delta \\ |e|^\alpha sign(e), |e| > \delta \end{cases} \tag{7}$$

To apply ADRC to the attitude control of small unmanned helicopter, we separate the whole model into two parts. One refers to the lateral variables (p and b), and the other refers to the longitudinal ones (q and a). To decouple these two parts, we design a second-order ADRC like Figure 2 for each part, where the structure of TD and ESO adopts equations (2) and (4). NLSEF is selected as the following nonlinear error combination:

$$u_0 = \beta_1 fal(e_1, 0.5, h) + \beta_2 fal(e_2, 0.25, h) \tag{8}$$

Because the original system inputs are coupled, the control value $\boldsymbol{u}$ needs to be transformed as:

$$\boldsymbol{u}_1 = \begin{bmatrix} A_{lat} & A_{lon} \\ B_{lat} & B_{lon} \end{bmatrix}^{-1} \boldsymbol{u} \tag{9}$$

Figure 2 Structure of ADRC

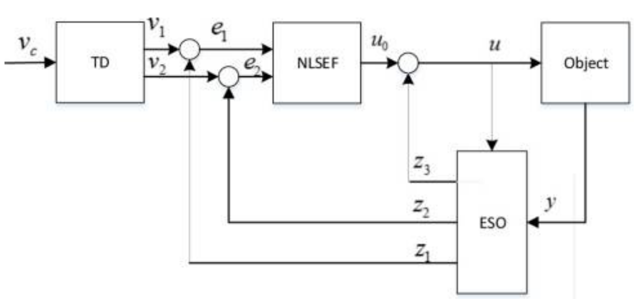

Levy flight-based pigeon-inspired optimization for active disturbance rejection control

Although ADRC is able to decouple original system and provides strong robustness, it is still not desirable under changeable circumstances because static parameters cannot be adjusted and coped with various situations. Hence, we need to adopt a group of adjustable parameters to optimize the ADRC performance. PIO is one of the newest swarm intelligence optimizations that is aimed to solve the problems of optimal searching. PIO imitates the process that homing pigeons find paths. It is similar to some bio-inspired algorithms such as PSO in the bionic mechanism. Compared with PSO, PIO could provide a wider search space and is more efficient on controller optimization.

Basic pigeon-inspired optimization algorithm

Just as the process of homing pigeons searching path, basic PIO algorithm can be divided into two stages and each step contains a relative operator (Duan and Qiao, 2014). At the first stage, map and compass operators are adopted which is inspired by the natural phenomenon that pigeons use the sun and magnetic particles to sense home direction in the beginning of flight. This operator is given as:

$$\begin{aligned} V_i(t) &= V_i(t-1) \cdot e^{-Rt} + rand \cdot (X_g - X_i(t-1)) \\ X_i(t) &= X_i(t-1) + V_i(t) \end{aligned} \tag{10}$$

where X_i and V_i are the position and velocity of pigeon i, R denotes map and compass factor, *rand* is a random number between 0 and 1 and X_g denotes the current global best position.

When the pigeons fly close to their destination, they will rely on landmarks neighboring them. Landmark operator manifests this process with the following model:

$$\begin{aligned} N_p(t) &= \frac{N_p(t-1)}{2} \\ X_c(t) &= \frac{\sum X_i(t-1) \cdot f_{\cos t}(X_i(t-1))}{N_p(t) \sum f_{\cos t}(X_i(t-1))} \\ X_i(t) &= X_i(t-1) + rand \cdot (X_c(t) - X_i(t-1)) \end{aligned} \tag{11}$$

where N_p is the number of available pigeons toward the destination with half decreasing in every iteration. This means half pigeons will follow the other available pigeons in the next search process. X_c is the center of available pigeons' position as the reference of the swarms which represents the landmark, and the function f_{cost} is the fitness function evaluating the quality of each pigeon. After these two steps, we can gain the convergent optimal solution.

Levy flight-based pigeon-inspired optimization

The basic PIO is more efficient than many homogeneous methods such as PSO and genetic algorithm. However, it also has some shortcomings to be improved such as the stochastic search space to be extended and the convergence speed to be accelerated. To improve the PIO algorithm, we introduce a novel Levy flight-based pigeon-inspired optimization (LFPIO) in which the two original operators are anew designed.

Levy flight search operator

Levy flight has been demonstrated that it is one of the best random walk models in which the step lengths have a probability distribution that is heavy-tailed (Barthelemy *et al.*, 2008). In the process of walking, the step lengths are subject to Levy distribution. The simplified Levy flight can be described as follows:

$$L(s) \sim |s|^{-\delta}, 1 < \delta \leq 3 \tag{12}$$

where s denotes random step length. When searching an unknown and large-scale space, Levy flight is more effective than Brown motion (Chakravarti, 2004) because the variance σ^2 of Levy flight increases more rapidly. The two kinds of variances are shown as follows:

$$\begin{aligned} &\sigma_B^2(s) \sim s && \text{Brown motion} \\ &\sigma_L^2(s) \sim s^{3-\delta}, 1 < \delta \leq 2 && \text{Levy flight} \end{aligned} \tag{13}$$

In Levy flight, some solutions execute local search, and others execute global search. This mechanism can balance the diversity and the convergence speed. At the same time, Levy flight can imitate the search behaviors of some animals such as the fish school and the pigeon flock. Hence, we use this mechanism to design the new search operator. Here, Levy flight can be implemented by Mantegna's algorithm (Mantegna and Stanley, 1994), and the operator can be described as following equations:

$$\begin{aligned} &s = \frac{\mu}{|v|^{1/\delta}} \\ &X_p = X_i(t-1) + s \cdot randn \cdot (X_i(t-1) - X_g) \\ &\mu \sim \mathrm{N}(0, \sigma_\mu^2), v \sim \mathrm{N}(0, \sigma_v^2), \delta = 1.5 \\ &\sigma_\mu = \left\{ \frac{\Gamma(1+\delta)\sin(\pi\delta/2)}{\Gamma[(1+\delta)/2]\delta \cdot 2^{(\delta-1)/2}} \right\}^{1/\delta}, \sigma_v = 1 \end{aligned} \tag{14}$$

where $\mathrm{N}(0, \sigma^2)$ denotes the normal distribution, s is the step length of Levy flight and *randn* is a random number subject to normal distribution. In addition, the elite selection strategy is utilized to improve the ability of local search and described by the following equation:

$$X_i(t) = \begin{cases} X_p, & \mathit{If} f_{\text{cost}}(X_p) < f(X_i(t-1)) \\ X_i(t-1), & \mathit{If} f(X_p) \geq f(X_i(t-1)) \end{cases} \tag{15}$$

Revised landmark operator

In basic PIO algorithm, the landmark operator can accelerate the convergence of algorithm. However, it easily leads to the premature convergence, and all solution will be trapped into local optima. To avoid the problem, we adopt the adaptive *Logsig* function to adjust the step length of search. Detailed equations are given as follows:

$$\begin{aligned} &Step = Logsig\left(\frac{N_{\max} \cdot \zeta - t}{k}\right) \\ &X_i(t) = X_i(t-1) + Step \cdot randn \cdot (X_g - X_i(t-1)) \end{aligned} \tag{16}$$

where ζ and k are the adaptive parameters of *Logsig* function which decides when the search converges, and $N_{\max}$ is maximum iterations.

Optimized active disturbance rejection control based on Levy flight-based pigeon-inspired optimization

The parameters of ADRC include r_0 from TD, $\beta_{01} \sim \beta_{03}$ from ESO and β_1, β_2 from NLSEF. We usually set $r_0 = 0.0001/h^2$ according to experiences, so the parameters to be optimized for each ADRC are the rest five. Before we execute LFPIO, the fitness function need to be confirmed. Here, we select the characteristics of step response including steady state error, input limitations and rise time to assess the whole system performance. The fitness function is listed as follows, we expect it as small as enough:

$$\begin{aligned} f_{\text{cost}} = &\int_0^\infty w_1(|e_1| + |e_2|)dt \\ &+ \int_0^\infty w_2(u_1^2 + u_2^2)dt + w_3(t_{r1} + t_{r2}) \end{aligned} \tag{17}$$

where w_1, w_2 and w_3 are the weight values, e and u are errors and input controls for each subsystem and t_r denotes the rise time. Because ADRC method could realize decoupling of the two attitude subsystems, the controller in each subsystem can execute parallelly. Due to each ADRC has five parameters, the dimension of total LFPIO is ten. When we test each solution, substitute the parameters into ADRC process and set the step instruction. Then we can obtain the characteristics of step response in fixed period and, hence, gain the relative fitness value. Figure 3 shows the structure of whole system.

The detailed implementation procedure of LFPIO for ADRC optimization is described as follows:

Figure 3 System with optimized ADRC

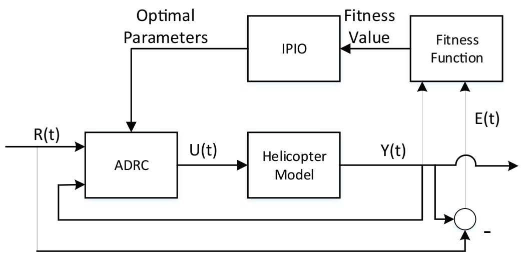

- *Step 1*: According to the control requirement, confirm the step size *h* and implementation period *T* of ADRC. Initialize the step command and state variables of small unmanned helicopter.
- *Step 2*: Initialize parameters of LFPIO, such as search space dimension *D*, maximum iterations $N_{\max}$, the pigeon population size *L*, weight values of fitness function and other relative parameters ζ and *k*.
- *Step 3*: Set each pigeon with a random position and substitute the solutions into ADRC, then compute the corresponding fitness function. Compare the fitness values and find the current best solution.
- *Step 4*: Update the position of each pigeon with Levy flight operator, then compare all the new fitness values to find the best solution.
- *Step 5*: Using the revised landmark operator to proceed the convergence of global optima and update each pigeon's position by equation (14).
- *Step 6*: If the ordinal of iteration Nc is greater than maximum iteration Nmax, stop and output the results. If not, go to *Step 4*.

The above steps can be summarized as a flowchart (Figure 4).

Comparative experiments

To investigate the feasibility and effectiveness of our proposed optimized ADRC with LFPIO, a series of comparative experiments with PSO and basic PIO are conducted. To verify the robustness of the whole system, some certain disturbances are considered.

The step instruction is set as one with step time zero. Select step length *h* as the sampling period 0.01 s and control period *T* as 1 s. Parameters of the helicopter model are given according to Ioannis *et al.* (2012). LFPIO maximum iteration $N_{\max}$ is 100, and according to the above, dimension *D* of total LFPIO is 10. The population of pigeons is 100 as the same number of candidate solutions. According to experiences, the five ADRC parameters can be adjusted in following ranges as β_{01} :[100,500], β_{02} :[100,1000], β_{03} :[1000,5000], β_1 :[1,20] and β_2 :[1,20]. After debugging, we select the parameters ζ and *k* in revised landmark operator as 0.5 and 15, respectively. To emphasize the control precision and rapidity, we set the weight values $w_1 = 0.999$, $w_2 = 0.001$ and $w_3 = 0.2$. To verify the effectiveness of LFPIO, the same parameters are adjusted in basic PIO and PSO, so the comparative results are obtained in Figures 5 to 7. In addition, an unexpected impulse wind disturbance with 6N·m and a stochastic wind disturbance with magnitude of 2N·m are added to the simulation experiments.

Figure 5 shows the average fitness value curves of LFPIO, basic PIO and PSO in 50 experiments. We select a group of parameters with best fitness values listed in Table I and test the step responses with these parameters shown in Figure 6 and 7. To demonstrate the precision of ESO, tracking curves of unknown dynamics containing wind disturbances in the lateral channel are shown in Figure 8.

From Figure 5, it is obvious that the proposed LFPIO converges more quickly and is more stable than basic PIO and PSO. Meanwhile, LFPIO is more reliable in global optima searching because of its extended search space. Moreover, we

Figure 4 General flowsheet of LFPIO

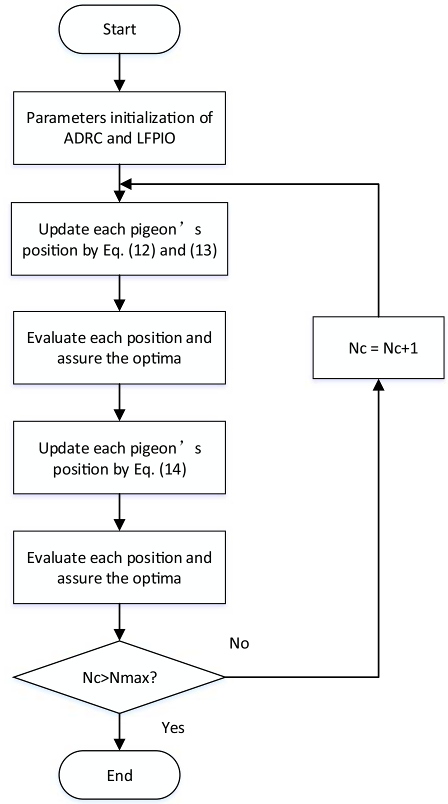

Figure 5 Comparative evolutionary curves of LFPIO, basic PIO and PSO

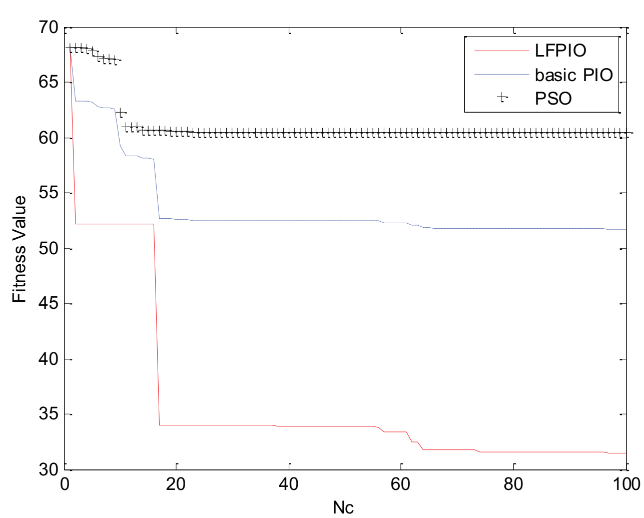

Figure 6 Comparative lateral step responses of optimized ADRC

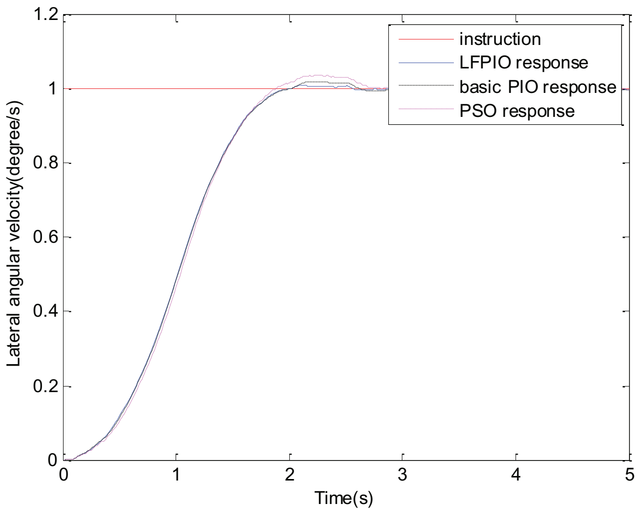

Figure 7 Comparative longitudinal step responses of optimized ADRC

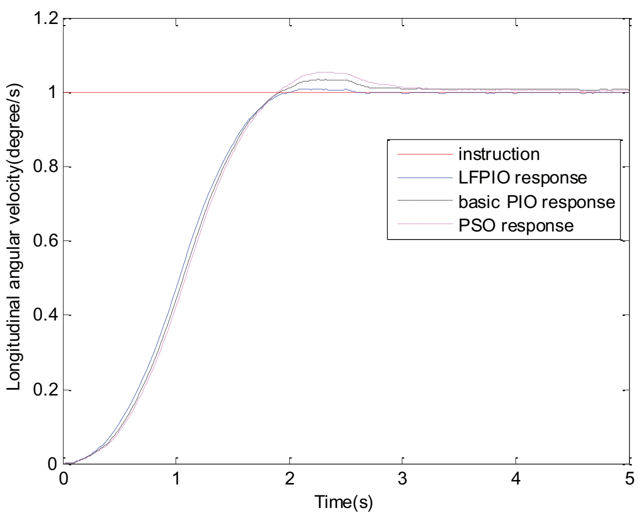

Table I Comparative optimal parameters in lateral model

Algorithms	Parameters					
	β_{01}	β_{02}	β_{03}	β_1	β_2	f_{cost}
LFPIO	155	350	4,480	13	15	32.6
PIO	212	653	3,080	8	11	52.3
PSO	119	833	3,760	12	14	61.3

can conclude from Figures 6 to 8 that ESO can estimate the unknown dynamics and support the optimized ADRC to execute real-time disturbance compensation for ideal control, so this system could provide proper responses under hard conditions. Among the optimized parameters, LFPIO-based ones respond more effectively.

Conclusions

This paper presents an ADRC method applied to small unmanned helicopters. A linear attitude model based on

Figure 8 Unknown dynamics observation by LFPIO-based ESO

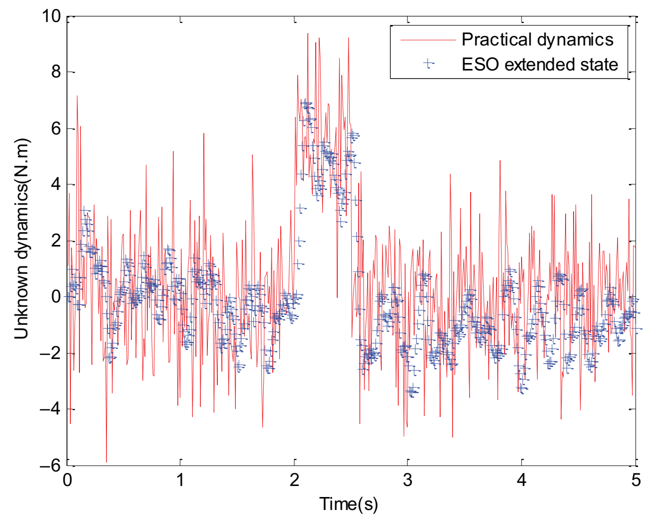

hovering state and small perturbation linearization is given in this work. To realize decoupling and strong robustness of the whole system, a couple of ADRCs are arranged into two subsystems. Moreover, to promote the efficiency of each basic ADRC, a novel LFPIO algorithm is developed to optimize the five adaptive ADRC parameters. To extend the search space and proceed the convergence speed, the two original operators of basic PIO are replaced. The comparative simulation experiments with basic PIO and PSO show that the proposed LFPIO can give the good precision and stability of convergent globally optimal solution. Besides, ADRC system with LFPIO-based optimal parameters could provide the best tracking precision and lowest overshoots under certain disturbances.

In the future, we expect that our optimized ADRC could be used in practical flight and our proposed LFPIO could be applied and developed in other important optimization aspects.

References

An, A., Wang, J., Zhang, H. and Yang, G. (2015), "Dynamics analysis of a microbial fuel cell system and PID control of its power and current based on the critical proportion degree method", *Environmental Engineering and Management Journal*, Vol. 14 No. 8, pp. 1821-1828.

Barthelemy, P., Bertolotti, J. and Wiersma, D.S. (2008), "A Levy flight for light", *Nature*, Vol. 453 No. 7194, pp. 495-498.

Bassrei, A. and Santos, E. (2007), "L- and Θ-curve approaches for the selection of regularization parameter in geophysical diffraction tomography", *Computers & Geosciences*, Vol. 33 No. 5, pp. 618-629.

Cai, G., Chen, B.M., Dong, X. and Lee, T.H. (2011), "Design and implementation of a robust and nonlinear flight control system for an unmanned helicopter", *Mechatronics*, Vol. 21 No. 5, pp. 803-820.

Cao, Y., Zhang, G. and Su, Y. (2004), "Mathematical modeling of helicopter aerobatic maneuvers", *Aircraft Engineering and Aerospace Technology*, Vol. 76 No. 2, pp. 170-178.

Chakravarti, N. (2004), "Beyond Brownian motion: a levy flight in magic boots", *Resonance*, Vol. 9 No. 1, pp. 50-60.

Aircraft Engineering and Aerospace Technology: An International Journal
Volume 89 · Number 6 · 2017 · 946–952

Deng, Y. and Duan, H. (2016), "Control parameter design for automatic carrier landing system via pigeon-inspired optimization", *Nonlinear Dynamics*, Vol. 85 No. 1, pp. 1-10.

Duan, H. and Qiao, P. (2014), "Pigeon-inspired optimization: a new swarm intelligence optimizer for air robot path planning", *International Journal of Intelligent Computing and Cybernetics*, Vol. 7 No. 1, pp. 24-37.

Duan, H. and Wang, X. (2016), "Echo state networks with orthogonal pigeon-inspired optimization for image restoration", *IEEE Transactions on Neural Networks and Learning Systems*, Vol. 1, doi: 10.1109/TNNLS.2015.2479117.

Duan, H., Luo, Q., Ma, G. and Shi, Y. (2013), "Hybrid particle swarm optimization and genetic algorithm for multi-UAVs formation reconfiguration", *IEEE Computational Intelligence Magazine*, Vol. 8 No. 3, pp. 16-27.

Han, J. (2009), "From PID to active disturbance rejection control", *IEEE Transactions on Industrial Electronics*, Vol. 56 No. 3, pp. 900-906.

Ho, H.F., Wong, Y.K. and Rad, A.B. (2008), "Direct adaptive fuzzy control for a nonlinear helicopter system", *Aircraft Engineering and Aerospace Technology*, Vol. 80 No. 2, pp. 124-128.

Ioannis, A.R., Kimon, P.V. and George, J.V. (2010), "Linear tracking control for small-scale unmanned helicopters", *IEEE Transactions on Control Systems Technology*, Vol. 20 No. 4, pp. 995-1010.

Ismaila, B., Tijani, R., Akmeliawati, A., Legowo, A., Budiyono, A.G., Abdul, M. (2011), "H∞ robust controller for autonmous helicopter hovering control", *Aircraft Engineering and Aerospace Technology*, Vol. 83 No. 6, pp. 363-374.

Kushwah, M. and Patra, A. (2014), "PID controller tuning using Ziegler-Nichols method for speed control of DC motor", *International Journal of Scientific Engineering and Technology Research*, Vol. 3 No. 13, pp. 2924-2929.

Lu, H., Liu, C., Guo, L. and Chen, W. (2015), "Flight control design for small-scale helicopter using disturbance-observer-based backstepping", *Journal of Guidance, Control and Dynamics*, Vol. 38 No. 11, pp. 2235-2240.

Mantegna, R.N. and Stanley, H.E. (1994), "Stochastic process with ultraslow convergence to a Gaussian: the truncated Levy flight", *Physical Review Letters*, Vol. 73 No. 22, pp. 2946-2949.

Nodland, D., Zargarzadeh, H. and Jaqannathan, S. (2013), "Neural network-based optimal adaptive output feedback control of a helicopter UAV", *IEEE Transactions on Neural Networks and Learning Systems*, Vol. 24 No. 7, pp. 1061-1073.

Qiu, H., Wei, C., Dou, R. and Zhou, Z. (2015), "Fully autonomous flying: from collective motion in bird flocks to unmanned aerial vehicle autonomous swarms", *Science China Information Sciences*, Vol. 58 No. 128201, pp. 1-3.

Sheng, S., Sun, C., Duan, H., Jiang, X. and Zhu, Y. (2014), "Longitudinal and lateral adaptive flight control design for an unmanned helicopter with coaxial rotor and ducted fan", *Proceedings of the 33rd Chinese Control Conference, Nanjing, 28-30 July*, pp. 130-135.

Shi, Y., Hou, C. and Su, H. (2008), "Auto-disturbance-rejection controller design based on particle swarm optimization algorithm", *Journal of System Simulation*, Vol. 20 No. 2, pp. 433-436.

Tang, S., Zheng, Z., Qian, S. and Zhao, X. (2014), "Nonlinear system identification of a small-scale unmanned helicopter", *Control Engineering Practice*, Vol. 25 No. 1, pp. 1-15.

Tang, S., Yang, Q., Qian, S. and Zheng, Z. (2015), "Height and attitude active disturbance rejection controller design of a small-scale helicopter", *Science China Information Sciences*, Vol. 58 No. 3, pp. 1-17.

Yang, F., Chen, Z. and Wei, C. (2013), "Nonlinear system modeling and identification of small helicopter based on genetic algorithm", *International Journal of Intelligent Computing and Cybernetics*, Vol. 6 No. 1, pp. 45-61.

Zhang, B. and Duan, H. (2016), "Three-dimensional path planning for uninhabited combat aerial vehicle based on predator-prey pigeon-inspired optimization in dynamic environment", *IEEE/ACM Transactions on Computational Biology and Bioinformatics, Beijing*, doi: 10.1109/TCBB.2015.2443789.

About the authors

Daifeng Zhang received his MSc degree in Control Science and Engineering from Beihang University (formerly Beijing University of Aeronautics and Astronautics, BUAA) in 2016. He is currently a PhD candidate with the School of Automation Science and Electrical Engineering, Beihang University. He is a Member of BUAA Bio-inspired Autonomous Flight Systems (BAFS) Research Group. His current research interest includes advanced flight control, bio-inspired computation and embedded system development.

Haibin Duan is currently a full Professor at School of Automation Science and Electrical Engineering, Beihang University (formerly Beijing University of Aeronautics and Astronautics, BUAA), Beijing, China. He received the PhD degree from Nanjing University of Aeronautics and Astronautics (NUAA) in 2005. He was an Academic Visitor of National University of Singapore (NUS) in 2007, a Senior Visiting Scholar of The University of Suwon (USW) of South Korea in 2011. He is currently an IEEE Senior Member and IFAC TC7.5 Technical Committee Member. He has published 3 monographs and over 60 peer-reviewed papers in international journals. His current research interests include bio-inspired computation, advanced flight control and biological computer vision. Haibin Duan is the corresponding author and can be contacted at: hbduan@buaa.edu.cn

Yijun Yang is currently a BSc candidate in the School of Automation Science and Electrical Engineering, Beihang University (formerly Beijing University of Aeronautics and Astronautics, BUAA). He is a Member of BUAA Bio-inspired Autonomous Flight Systems (BAFS) Research Group. His current research interests include computational intelligence techniques and their applications.